

There and (slowly) back again: Entropy-driven hysteresis in a model of DNA overstretching

Stephen Whitelam, Sander Pronk and Phillip L. Geissler

Department of Chemistry, University of California at Berkeley, Berkeley CA 94720
83

*Physical Biosciences and Materials Science Divisions,
Lawrence Berkeley National Laboratory, Berkeley, CA 94720*

December 2, 2024

DNA *in vivo* experiences protein-mediated tensile forces large enough to alter the structure and stability of the hybridized state. Experiments show that double-stranded DNA, when pulled along its axis, elongates abruptly at a force of about 65 pN. Two physical pictures have been developed to describe this overstretched state of DNA. The first introduces a new hybridized phase, called S-DNA, structurally and thermodynamically distinct from standard B-DNA. The second picture proposes that strong forces simply induce a phase transition to a molten state consisting of unhybridized single strands. Little thermodynamic evidence exists to discriminate between these competing pictures. Here we show that within a microscopic model of DNA, the kinetics associated with these two pictures are very different. The nonextensive entropy of unhybridized regions in our model produces hysteresis in a cycle of overstretching and relaxing whenever melting is substantial. Since hysteresis is observed in experiments only at high temperatures, our study requires the proposed S form of DNA in order to account for overstretching kinetics at low temperature.

The thermodynamics of in-vitro DNA pulling experiments does not conclusively establish the nature of the overstretched state. The abruptness of elongation suggests that the extended form repre-

sents a thermodynamic phase different from B-DNA. The picture of overstretching as a transition to S-form DNA, a putative hybridized state 1.7 times longer than B-DNA [1, 2, 3, 4, 5, 6], is motivated by the mechanical properties of the overstretched state. The latter has a stretch modulus of about 1600 pN/0.34 nm [2], which exceeds the stretch moduli of both B-DNA (~ 1300 pN/0.34 nm) and unhybridized forms of DNA at comparable extensions. The competing picture, which considers overstretching to be a force-induced ‘melting’ to unhybridized single strands [7, 8, 9, 10], is bolstered by the dependence of the overstretching force on parameters like pH and ionic strength [9, 1, 2]; these parameters are known to change the melting temperature of the molecule at zero tension. In addition, the binding of ethidium to DNA increases the overstretching force in a manner consistent with data from thermal melting studies [9].

Here we show that these thermodynamic data can be used to guide a model of DNA able to distinguish *dynamically* between the two pictures. We have constructed such a model of DNA, with a resolution of one base-pair, whose kinetics we explore under pulling conditions similar to those used in experiments. We allow each base-pair to instantaneously adopt one of three discrete states: a standard helical state (B), a molten state (M) of two load-bearing strands, and an overstretched double-stranded state

(S). Within computer simulations of the model, we demonstrate that omitting S-DNA leads to kinetics not in accord with experiment.

The most striking kinetic effect observed in experiment is hysteresis at high temperature (e.g. above 30°C for λ -DNA at 500 mM NaCl concentration [11]) in force-extension data for the stretching and subsequent shortening of a pair of initially hybridized DNA molecules. This has been ascribed to the ‘unpeeling’ and slow reattachment of one strand from the other, beginning from nicks in the phosphate backbone [2]. We verify that such hysteresis is generated within our model when we allow unpeeling in the presence of nicks, but here we show that there exists an alternative mechanism that generates hysteresis. This mechanism originates in the entropy-driven metastability of molten bubbles.

The entropy associated with molten regions of DNA does not grow linearly with the number of consecutive unhybridized bases. A ‘bubble’ of n unpaired bases constitutes a loop of single-stranded DNA (ss-DNA) of length $2n$, whose entropy has a nonextensive contribution $\Delta S(n) = -k_B c \ln(2n)$ [12, 13]. This nonextensivity is responsible for the sharpness of the thermal melting transition in long DNA molecules. Pinching a bubble in its middle incurs a statistical penalty $\sim n^{-c}$. A positive loop exponent c therefore favours large bubbles over multiple smaller ones, rendering the melting transition sharp. This bubble-pinching penalty has a direct consequence for the kinetics in our pulling simulations. Because for large bubbles pinching is rare, and the closing of a bubble from its ends is a slow process, large molten bubbles can resist closure for times comparable to that of stretching. This can prevent the molecule from reaching equilibrium, thereby rendering the stretching and shortening cycle hysteretic. The degree of hysteresis depends strongly on the value of the loop exponent c . Estimates for the latter under zero tension range from ~ 1.8 [13] to ~ 2.1 [14]. A calculation similar to that of Ref. [12] (see Methods) shows that to a first approximation the loop exponent c is not altered by tension.

As a consequence of the association between melting and hysteresis, we find that without the S-phase, when overstretching corresponds to force-induced melting, considerable hysteresis is generated under

typical loading rates at *all* temperatures. We require the S-phase in order to explain the kinetics of low-temperature overstretching, which does not exhibit hysteresis.

To construct our model, we imagine dividing a pair of hybridized DNA molecules into sites of length equal to the distance along the backbone between adjacent base-pairs, ‘blurring out’ details on smaller scales. Each site is fixed to be of type AT or CG (we assume fully complementary strands), and at any instant adopts one of the forms M, S or B. In the presence of nicks, we allow also an ‘unpeeled’ state U. Such discrete models of biopolymers have a long history, beginning with the two-state model of Bragg and Zimm [15], used in the 1950s to study the melting transition of homopolymers. More elaborate discrete models of conformational transitions in DNA have since been considered, including the model of SantaLucia [16], and a static three-state model of overstretching [2]. These models allow one to make predictions on time and length scales (seconds, thousands of base-pairs) greatly in excess of those available to molecular dynamics techniques (microseconds, tens of base-pairs) [17], albeit at a lower level of detail.

In order to determine the statistical weight associated with each state, we note that they derive from molecular free energies of two types, force-dependent and force-independent. We shall describe the force-independent free energies first.

B-DNA possesses both base-pairing and stacking interactions, which we estimate from melting studies [16]. In addition, in B-DNA there exists a water-mediated interaction between each nucleotide and the opposing nucleotide four base-pairs distant. This interaction is due to the helical geometry, and is lost upon disruption of the helix [18, 19]. We account for this effect by assigning an interaction of strength $5k_B T_{310}$ [15, 2] between neighbouring B- and non-B sites.

We assume that the extended S state must lose some of the short-ranged stacking energy, and we determine this loss by requiring phase coexistence between the B and S phases at a pulling force of 65 pN. We note that Zhou and Ou-Yang have attempted to quantify this loss from first principles [6].

The statistical weight of the M-phase receives a

contribution from the extensive entropy of melting (at zero force), which we obtain from thermal data [7, 16]. We augment this entropy with the nonextensive correction $\Delta S(n)$. The latter amounts to a long-ranged interaction.

We determine the force-dependent free energies by integrating, as a function of pulling force, the experimentally-measured extension of each phase. The behaviour of B-DNA in the regime of interest is described by an extensible worm-like chain model [20], with contour length 0.34 nm/bp, persistence length 50 nm, and force constant 1300 pN/0.34 nm. We assume that S-DNA can be similarly parameterized, with a contour length 0.58 nm/bp, and a force constant 1600 pN/0.34 nm. Lacking experimental measurements of S-DNA flexibility, we assume its persistence length to be equal to the persistence length of B-DNA. We take the mechanics of M-DNA to be that of two pieces of load-bearing ss-DNA. For the latter, we adopt the phenomenological parameterization of Ref. [2], appropriate for varying salt concentration.

To model nicked DNA we add to our model a fourth state, called unpeeled (U) [2]. We take the entropy of this state to be that of M-DNA without the loop correction, and we assume its elastic response to be that of a single, load-bearing strand. Any unhybridized site connected to at least one nicked site by an unbroken region of unhybridized sites is considered unpeeled; if not so connected, it is molten.

With the thermodynamics of our model thus determined, we investigate its predictions for the kinetics of overstretching. We use a Monte Carlo (MC) dynamics designed to mimic pulling at a constant speed, appropriate for experiments carried out using optical tweezers. We calculate the molecular tension f by assuming that the molecule and optical trap remain in mechanical equilibrium, the sum of both extensions changing linearly with time. We set the loading rate during shortening equal and opposite to that during stretching.

We first discuss the dynamics of the full model, which includes the S-state, both with nicks and without. Throughout, we assume that un-nicked systems are nevertheless torsionally unconstrained.

A typical experiment consists of elongating λ -phage DNA at a constant rate until it overstretches.

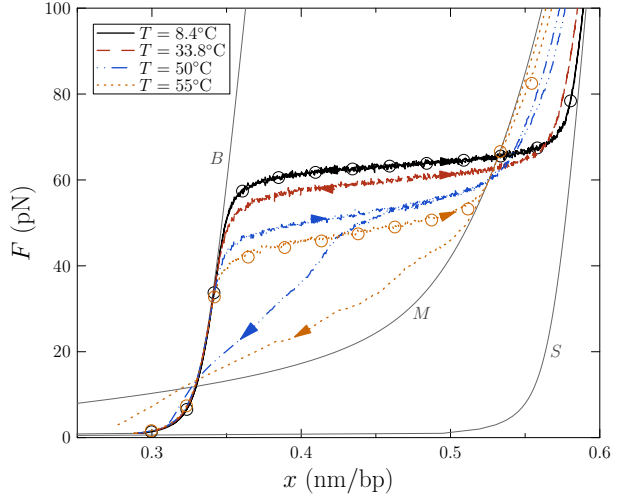


Figure 1: Effect of temperature. Theoretical force-extension data for un-nicked λ -phage DNA at 150 mM NaCl and pulling rate 200 nm/s. We show data for $T = 8.4^\circ\text{C}$, 33.8°C , 50°C and 55°C (top to bottom), with loop exponent $c = 2.1$, together with equilibrium data for 8.4°C and 55°C (symbols). At low temperature, overstretching is a transition from B- to S-DNA. Increasing temperature causes melting, resulting in a drop in plateau height. At higher temperatures still, melting prevents the molecule from reaching equilibrium during the shortening transition, generating hysteresis. The overstretched state at high temperature is largely M-DNA. The grey lines show equilibrium force-extension data for the states B, S and M. The kinetic data at each temperature are from a single, representative trajectory.

Once overstretched, the elongation is reversed, allowing the molecule to recover its original contour length. Force-extension data show two striking effects as the ambient conditions are altered so as to reduce the stability of the hybridized state with respect to the unhybridized state, either by reducing salt concentration [1] or by increasing temperature [11]. The first effect is a reduction in the force required to overstretch the molecule, causing the force-extension plateau to drop. The second effect, which occurs as the hybridized state is further destabilised, is the development of hysteresis in force-extension data. In-

triguingly, this hysteresis is asymmetric: the overstretching transition exhibits a force-extension response similar to the response seen at higher salt concentrations or lower temperatures; the shortening transition, by contrast, occurs at (often substantially) lower forces.

We observe both effects in simulations. In Figure 1 we show data for un-nicked λ -DNA, at varying temperature and fixed salt concentration (150 mM NaCl), similar to the protocol employed in Ref. [11]. At low temperatures, well below the zero-tension melting point at this salt concentration ($T_m \approx 72^\circ\text{C}$) the hybridized state is stable with respect to the unhybridized state over the full range of force. As determined by the thermodynamics, we observe a transition from a B-rich to an S-rich phase above the B-to-S overstretching force of 65 pN. At moderate temperatures, melting causes the overstretching force to drop. M-DNA is longer than B-DNA at tensions ≥ 10 pN, and so becomes increasingly favoured thermodynamically as tension increases. Force-induced melting can thus occur at temperatures well below the zero-tension melting temperature, causing elongation of the molecule. At sufficiently large temperature this elongation occurs at forces lower than 65 pN, causing the plateau to drop.

At still higher temperatures, kinetic effects manifest themselves in the guise of asymmetric hysteresis, as the stretching transition remains in equilibrium while the shortening transition does not. This hysteresis is driven by the development of large molten bubbles, via the following mechanism. At sufficiently large tension, molten DNA nucleates and spreads. The nonextensive bubble entropy rewards bubble coalescence, leading to the formation of large bubbles. During shortening, as the tension falls, B-DNA becomes thermodynamically favoured over M-DNA. However, because of the bubble-pinchning penalty, the nucleation of B-DNA in M-DNA is suppressed kinetically. Large molten bubbles thus close in general from their ends. Because this is a gradual process, requiring a collective relaxation over often large distances, such bubbles can persist far into the shortening transition, preventing the molecule from reaching equilibrium (see Methods for an illustration of the slow dynamics of melting).

Typically, hysteresis in experiments sets in at tem-

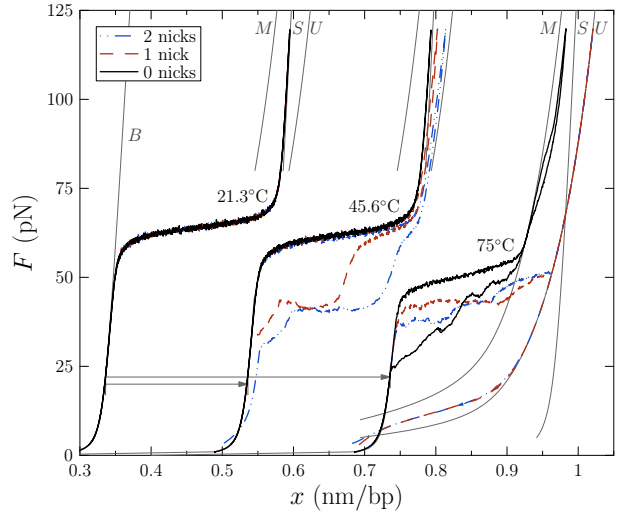


Figure 2: Effect of temperature in the presence of nicks. Theoretical force-extension curves for λ -phage DNA at 500 mM NaCl pulled at 100 nm/s with no nicks (black), 1 nick (red), or 2 nicks (blue). The loop exponent is $c = 2.1$. We show data for $T = 21.3^\circ\text{C}$, 45.6°C and 75°C , offset horizontally. Unpeeling-driven hysteresis sets in at lower temperatures than does melting-driven hysteresis, but at higher temperatures both mechanisms operate. At high temperature, the overstretched state of a nicked molecule is largely unpeeled DNA, and proceeds via two (one nick) or three (two nicks) plateaux. Without nicks, the high- T overstretched state is molten, and so shorter than the nicked structures. We show equilibrium force-extension data for the states B, S, M and U (grey lines).

peratures lower than does melting hysteresis in our simulations. For example, considerable hysteresis develops in experiment at temperatures in the $30-45^\circ\text{C}$ range for λ -phage DNA at 500 mM NaCl [11], a salt concentration at which the hybridized state is considerably more stable ($T_m \approx 95^\circ\text{C}$) than at 150 mM, the conditions used to generate Fig 1. We believe that this hysteresis, and indeed most experimental hysteresis seen thus far, can be ascribed to unpeeling from nicks, as has been previously suggested [1, 2, 7]. In Figure 2 we show force-extension data at varying temperature for λ -DNA at 500 mM NaCl, with 0, 1

or 2 nicks. At high temperature, the overstretched state is in the absence of nicks mostly molten, and in the presence of nicks mostly unpeeled. Kinetically, we find that unpeeling-driven hysteresis develops at lower temperatures than does melting-driven hysteresis, because at a given force the unpeeled state is longer than the molten state. The free energy of the former can fall below that of the B-state at a lower force than can the latter. There is therefore a range of T and f for which unpeeling can cross CG regions (and therefore proliferate over long distances), while melting cannot. At higher temperatures, when M-DNA can proliferate, both mechanisms drive hysteresis; the relative importance of unpeeling to the observed hysteresis increases with the nick density.

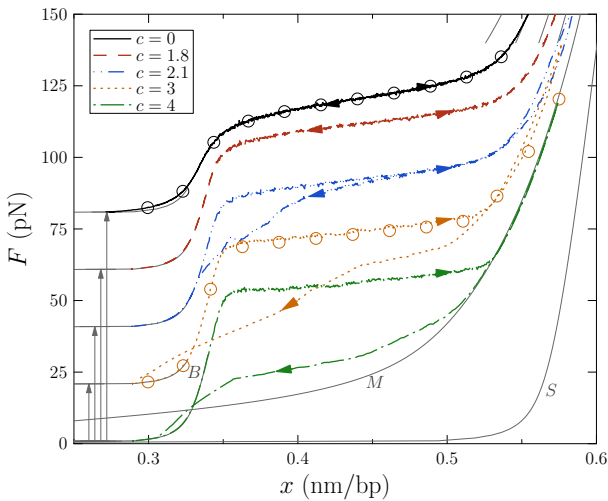


Figure 3: Effect of varying loop exponent. Theoretical force-extension curves for un-nicked λ -phage DNA at 150 mM NaCl, $T = 50^\circ\text{C}$, and pulling rate 200 nm/s. The curves are for loop exponents $c = 0, 1.8, 2.1, 3$ and 4 (offset vertically), and we show equilibrium data for $c = 0$ and $c = 3$ (symbols). The hysteresis at fixed pulling rate vanishes as c decreases, even though the *equilibrium* fraction of M-DNA increases. Note that the ‘cooperativity’ (or sharpness) of the overstretching (here largely force-induced melting) transition decreases as c decreases.

The degree of melting-driven hysteresis is strongly dependent upon the value of the loop exponent c . To

illustrate this point, we show in Figure 3 theoretical force-extension data generated under similar conditions to those used for Fig. 1: un-nicked λ -DNA at 150 mM NaCl and $T = 50^\circ\text{C}$. Here we vary the loop exponent c . While increasing c decreases the *equilibrium* fraction of M-DNA, it makes very slow the dynamics of large molten bubbles, and leads to greater hysteresis. The extent of the hysteresis is a sensitive function of c , offering the possibility of testing the effective value of c by comparing work distributions from pulling experiments for un-nicked molecules with simulation data.

Our model predicts that melting-driven hysteresis should be observed under conditions favouring the development of large molten bubbles. In addition to temperature and salt, both loop entropy and base-pair sequence have a striking effect on the size and stability of bubbles, as is revealed by examining a system’s microscopic configuration as a function of time. We show in Figure 4 representative data of this nature for a small, un-nicked molecule. A large value of the loop exponent c promotes large bubbles, as do sequences with large AT-rich regions. In a system segregated into halves of pure CG and AT content, the AT region melts entirely at high force, and remains molten for the duration of the simulation.

We have demonstrated that within our model, hysteresis (at typical experimental pulling rates) is intimately associated with melting. A natural consequence of this association is that without the S-state, where overstretching is a transition to unhybridized DNA [7, 8], considerable hysteresis is generated, regardless of temperature. In Figure 5 we show the predictions of our model with the S-phase suppressed. We find that at all temperatures the overstretching plateau height varies continuously with temperature, and at typical experimental loading rates considerable hysteresis develops because of large-scale melting. Provided that c is not changed substantially by pulling, these results are not in agreement with experiment, where hysteresis is seen only at high temperatures.

The quantitative behaviour of our model is very sensitive to the details of its thermodynamic parameters. The observed hysteresis is strongly dependent upon c , which although unchanged by pulling within a simple random walk model (see Methods), may suf-

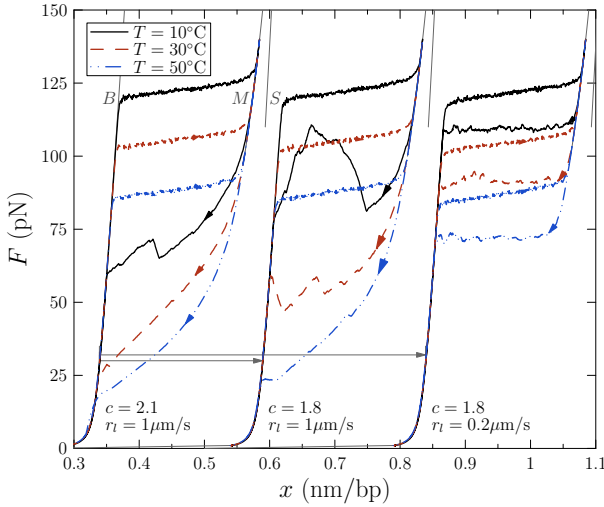


Figure 5: Effect of suppressing the S-phase. Theoretical force-extension curves for un-nicked λ -phage DNA at 1M NaCl concentration. Overstretching corresponds to force-induced melting. We show three data sets, for combinations of loop exponents $c = 2.1$ and $c = 1.8$, and loading rates $r_l = 1000$ nm/s and $r_l = 200$ nm/s. The curves in each set correspond to $T = 10^\circ\text{C}$, 30°C and 50°C (top to bottom). The onset of overstretching depends on the free energy difference between B- and M-DNA. This quantity varies continuously with temperature, and so therefore does the plateau height. The complete melting of the system generates large-scale hysteresis at all temperatures, for both loading rates. The ‘sawtooth’ response is caused by the molecule shortening suddenly at fixed total extension. The optical trap ‘spring’ is forced to lengthen, and the system follows a diagonal line whose gradient is the negative of the trap spring constant.

fer corrections when self-avoidance and interaction effects are accounted for. We have also assumed that the B-to-S forces for AT and CG sections are equal. This is likely not the case [1, 7, 22], but conclusive data do not yet exist.

However, the important qualitative features of our model are robust to changes in the details of its parameters. In particular, hysteresis induced by the slow dynamics of melting is also pronounced if we

take an alternative form for the nonextensive entropy of molten regions, $\Delta S(n) = -k_B c \ln(1 + n)$ [24], and the dynamics of our model is insensitive to a change from the Glauber to the Metropolis Monte Carlo acceptance rate.

We have studied the kinetics of a simple model of the DNA overstretching transition, whose thermodynamics we obtain from experimental thermal and elastic data. We have compared the kinetic predictions associated with two pictures of overstretching, one which postulates the existence of an extended hybridized state of DNA, the other considering overstretching to be force-induced melting. Each picture explains key features of the thermodynamics of overstretching. Using a kinetic Monte Carlo scheme designed to mimic pulling under a constant rate of extension, we have shown that temperature-dependent hysteresis can be generated by melting, as well as by the unpeeling of one strand from the other. Our model implies that a solely force-induced melting transition would be hysteretic at all temperatures at typical loading rates, an observation not supported by experiment. Our results are consistent with the idea that overstretching is at low temperature a transition to a double-stranded state, with a combination of melting and unpeeling becoming increasingly important, kinetically and thermodynamically, as temperature is raised.

A key prediction of our model is that the overstretching-shortening cycle for *un-nicked* but torsionally unconstrained DNA should display temperature-dependent hysteresis at high temperature. The elimination of nicks is necessary to remove the hysteresis associated with unpeeling. If this prediction is verified by experiment, it would provide evidence that melting can generate hysteresis, thereby offering a means of distinguishing between the two pictures of DNA overstretching based on their *kinetic* predictions. In addition, it would imply that large, metastable molten bubbles can develop in overstretched DNA, which may have significance for its biological function.

1 Methods

Approximate entropy of loops under tension. The en-

tropy associated with molten DNA has been shown to be important during overstretching from the strong temperature dependence of the overstretching force [9]; from theoretical fits to experimental data [23]; and from molecular dynamics simulations [17]. Associated with the extensive entropy of melting is a nonextensive penalty for closing a loop, which to a first approximation may be calculated in the following manner [12].

Consider an ideal random walk of n steps on a d -dimensional hypercubic lattice, constrained to return to its origin. Because the loop closes, the number of steps in the + and - directions in each dimension must be equal; the number of ways of ordering m such steps in one dimension is $W(m) \equiv m!/(m/2)!)^2$. Consider a walk in which $rn < n$ steps are taken in a favoured dimension, corresponding to the direction of pulling. The case $r = 1/d$ is an unbiased walk. If the remaining $(1-r)n$ steps are distributed equally amongst the other $d-1$ dimensions, then the entropy of the walk is

$$S(n, r) = k_B \ln W(rn) + (d-1)k_B \ln W(\alpha n). \quad (1)$$

We have defined $\alpha \equiv (1-r)/(d-1)$. The first term in Equation (1) accounts for the number of ways of ordering the steps in the ‘pulling’ dimension; the second accounts for the steps in the other $d-1$ dimensions. Equation (1) can be approximated by Stirling’s formula as

$$S(n, r) \approx k_B n \ln 2 - k_B c_0 \ln n_r. \quad (2)$$

The first term in Equation (2) is the extensive entropy accounting for the 2 choices (+/-) for each of the n steps of the walk. The second term is the nonextensive penalty for loop closure. The dependence upon aspect ratio r is confined to the effective loop length parameter $n_r \equiv \frac{1}{2}\pi r^{1/d} \alpha^{1-1/d} n$. The exponent $c_0 \equiv d/2$ does not depend on r . Under zero tension, in $d = 3$, this value is increased to ~ 1.8 by the constraint of self-avoidance [13], and further to ~ 2.1 if loop interactions are taken into account [14]. We do not address these effects here.

The effect of stretching is to *increase* the entropy of a loop, by decreasing the penalty associated with closing the loop. Crucially, this change in entropy is independent of the length of the loop, and can be regarded

as a constant correction for all loops, large or small. Numerically, this correction is small. For $d = 3$, doubling the aspect ratio of a loop in a given dimension causes an increase in the entropy of a loop of length n of $S(n, r = 2/3) - S(n, r = 1/3) \approx k_B \ln \sqrt{2}$. This is smaller in magnitude for all n than the nonextensive portion $-k_B c_0 \ln(2n)$.

Model thermodynamics. To caricature the λ -phage DNA used in experiments [21, 11] we use systems of size $N = 4 \times 10^4$, segregated into a left half with AT content 45% (chosen with Poisson probability), and a right half with AT content 55%. We denote base *type* by the variable $\gamma \in \{\text{AT,CG}\}$, and *state* by the variable $\alpha \in \{\text{M,S,B,U}\}$.

The Hamiltonian of our model is $\mathcal{H} = \sum_{i=1}^N (\mathcal{H}_l + \mathcal{H}_{nl})$, where the local piece reads

$$\begin{aligned} \mathcal{H}_l = & - [TS_m + w_M(f)] \delta_i^M \\ & - [\lambda_\gamma \epsilon_\gamma + w_S(f)] \delta_i^S \\ & - [\epsilon_\gamma + w_B(f)] \delta_i^B \\ & + \frac{1}{2} \epsilon_s \left(\delta_i^B \tilde{\delta}_{i+1}^B + \tilde{\delta}_i^B \delta_{i+1}^B \right). \end{aligned} \quad (3)$$

Here f is the molecular tension. We have introduced the variables δ_i^α and $\tilde{\delta}_i^\alpha$, which take the values 1 and 0 respectively when site i assumes the state α , and respectively 0 and 1 otherwise. The nonlocal piece accounting for the nonextensive entropy of molten sections is

$$\mathcal{H}_{nl} = \sum_{n=1}^{N-i} J_n \tilde{\delta}_{i-1}^M \tilde{\delta}_{i+n}^M \prod_{s=0}^{n-1} \delta_{i+s}^M \quad (4)$$

where $J_n \equiv cT \ln(2n)$.

In what follows we shall define the parameters of Eq. (3).

We approximate the base-pairing-stacking energies of B-DNA sites by assuming that these energies depend only upon the on-site base-pair type (AT or CG), and not the type of neighbouring sites. This approximation can be regarded as a ‘renormalization’ of the neighbour-dependent stacking energies of more detailed models [16], by dividing into two sets interactions containing 1) any A or T bases, or 2) any C or G bases. This level of detail is sufficient to capture the essence of sequence heterogeneity, namely the extra stability against de-hybridization of CG

over AT base-pairs, in free energy terms roughly $2 k_B T$ at 310K. It also allows us to capture the variation with AT content of the melting temperature of DNA. We fix the values of the energies ϵ_{CG} and ϵ_{AT} , and the extensive entropy of M-DNA, S_m , using thermal data. Specifically, we require that for a given salt concentration the mid-point of $f = 0$ melting curves for purely AT- and purely CG-DNA, with $c = 2$, reproduce values known from experiment [7, 16]. We take $(\epsilon_{\text{AT}}, \epsilon_{\text{CG}}) = (14.28, 15.64) + (0.81, 0.55) \ln M$ in units of $k_B T_{310}$ (we choose the extensive entropy of molten regions to be $S_m = 12.5 k_B$). Here M is the molar NaCl concentration. To fix the base-pairing-stacking energy $\lambda_\gamma \epsilon_\gamma$ of the S-state we require that it be in thermodynamic equilibrium with the B-state at an overstretching force $f_o = 65 \text{ pN}$: $w_B(f_o) + \epsilon_\gamma = w_S(f_o) + \lambda_\gamma \epsilon_\gamma$. Experiment [22] and theory [7] suggest that the overstretching forces for CG and AT sites may be different, but currently no consensus exists. The important qualitative features of our model are robust to variations in these forces. We obtain $(\lambda_{\text{AT}}, \lambda_{\text{CG}}) \approx (0.73, 0.76)$ at 310 K. The junction energy ϵ_s we set to $5 k_B T_{310}$.

The extensible worm-like chain expression for the extension per basepair x_ζ , $\zeta \in \{\text{B}, \text{S}\}$ as a function of chain tension f is given approximately by [20]

$$x_\zeta(f) = \bar{x}_\zeta \left(1 - \frac{1}{2} \left(\frac{k_B T}{f P_\zeta} \right)^{1/2} + \frac{f}{S_\zeta} \right). \quad (5)$$

We choose $(\bar{x}_S, \bar{x}_B) = (0.340, 0.578) \text{ nm}$, $P_S = P_B = 50 \text{ nm}$, and $(S_S, S_B) = (1300, 2730) \text{ pN}$. We bound the above expression (which breaks down at very small forces $f < 0.1 \text{ pN}$ [7]) from below by zero.

We use the phenomenological model of Ref. [2] for the elastic behaviour of ssDNA,

$$x_{\text{ss}}(f) = \bar{x}_{\text{ss}} \left(\frac{a_1 \log(f/f_1)}{1 + a_3 e^{-f/f_2}} - a_2 - \frac{f}{f_3} \right). \quad (6)$$

Here $\bar{x}_{\text{ss}} = 0.34 \text{ nm}$, $a_1 = 0.21$, $a_2 = 0.34$, $a_3 = 2.973 + 0.5129 \ln M$, $f_1 = 3.7 \times 10^{-3} \text{ pN}$, $f_2 = 2.9 \text{ pN}$, and $f_3 = 8000 \text{ pN}$. This formula accounts for the increase in persistence length of ssDNA under low salt conditions, which significantly affects the melting behaviour of the system at nonzero tension. We find that the extensible freely-joined chain fit to ssDNA [21], which does not account for the increase

in its persistence length at low salt, leads to larger melting temperatures at nonzero tension. We neglect the ‘pulling out’ at high forces of entropic degrees of freedom of ssDNA. Within the FJC model this effect is of order $\sim 1 k_B T_{310}$ per base-pair at 65 pN. We also neglect the effects of secondary structure, which for load-bearing strands we expect to be small.

The free energies of stretching are given by $w_\alpha(f) \equiv \int_0^f df' x_\alpha(f')$. We assume that M-DNA consists of two noninteracting, load-bearing strands, and so we take $x_M(f) = x_{\text{ss}}(f/2)$ and $w_M(f) = 2w_{\text{ss}}(f/2)$.

Model dynamics. We use a Monte Carlo dynamics designed to mimic experiments in which the extension of the molecule is changed at a constant speed. We impose a time-dependent global length $L(t)$ and compute the tension f . We impose fixed boundary conditions, with sites 1 and N constrained to be B-form. The relative extensions of the phases are fixed by the constraint of mechanical stability, $f = f_B(x_B) = f_S(x_S) = f_M(x_M)$, where the $f_\alpha(x)$ are found by inverting the $x_\alpha(f)$. The absolute extensions x_α are fixed by the requirement that the imposed extension equal the sum of the molecular and optical trap extensions, $L(t) = \sum_\alpha n_\alpha x_\alpha + f/k_t$, n_α being the number of sites of phase α . The term f/k_t describes the extension of the optical trap, which we assume to be an harmonic spring of constant k_t . We start each run from a fully helical configuration at some small global length L_0 , which implies $Nx_B(t=0) + f_B(x_B)/k_t = L_0$. This relation determines the initial molecular tension $f(t=0)$ and the initial extensions $x_\alpha(t=0)$. We equilibrate the system at this fixed, small extension before beginning the pulling protocol. To perform a pulling simulation we increment the global length according to $L(t) = v_0 t$, with t measured in units of N MC steps. An MC step consists of a proposed change in the state of a randomly chosen site, accepted with the Glauber probability. We enforce the condition of mechanical equilibrium by proposing once per MC step a change δf in the global tension, accepted if the quantity $\Delta \equiv |\sum_\alpha n_\alpha x_\alpha + f/k_t - L(t)|$ does not increase. To calibrate v_0 we assume a base opening rate of 10^8 s^{-1} [2]. We reverse the pulling rate ($v_0 \rightarrow -v_0$) when f exceeds 120 pN (140 pN in Fig. 5). Kinetic data are representative individual trajectories, selected at ran-

dom from a large number of such trajectories. Each equilibrium symbol (Figs. 1 and 3) was calculated from 5 independent simulations run at zero loading rate for 3.5×10^3 MC sweeps; error bars are smaller than the symbols.

Unpeeling. To model the unpeeling of one strand from another, we add to our model a fourth state U , with Hamiltonian $H_U = \sum_{i=1}^N \mathcal{H}_U$, where

$$\mathcal{H}_U = -[TS_m + w_U(f)] \delta_i^U. \quad (7)$$

We take the elastic response $w_U(f)$ to be that of a single strand. The dynamics of U-DNA is governed by the following rules. We allow unpeeling to start only from nicks, which we place randomly. We consider all nicks to be on the same strand, ensuring that one strand is always load-bearing. A nick consists of two neighbouring sites, i_- and i_+ . Unpeeling can proceed left from i_- and right from i_+ . Any unhybridized site connected to at least one nicked site by an unbroken region of unhybridized sites is considered unpeeled; if not so connected, it is molten. We allow non-local changes of state associated with a change in state of a single site. For example, pinching an unpeeled strand of length ℓ_1 at a position $\ell_2 < \ell_1$ from its end changes a region of length $\ell_1 - \ell_2$ from unpeeled to molten. If an unpeeled region advances from its starting nick to an adjacent nick, that unpeeled region is ‘frozen’ for the duration of the simulation, modeling the effect whereby stretching can render sections of multiply-nicked molecules irreversibly single-stranded.

Bubble thermodynamics. Relative to an identical length of B-DNA, an isolated molten bubble of length ℓ has (ignoring sequence heterogeneity) free energy

$$F(\ell) = (\epsilon - k_B T S_m) \ell + k_B T c \ln \ell + \epsilon_s. \quad (8)$$

The derivative of F with respect to ℓ changes sign at $\ell_{c.n.} = c(S_m - \epsilon/k_B T)^{-1}$. Bubbles of length $\ell > \ell_{c.n.}$ grow, while smaller bubbles shrink. We can therefore regard $\ell_{c.n.}$ as the size of a critical nucleus of M-DNA. In this isolated-bubble approximation, $\ell_{c.n.}$ diverges at $T_c \equiv \epsilon/k_B S_m$.

Bubble dynamics. In Figure 6 we illustrate the slow dynamics associated with melting (see also Ref. [25]). From microscopic configurations as a function of time, we see that in heating-cooling cycles, a large loop exponent c induces an asymmetry in melting-hybridization dynamics. This asymmetry manifests

itself as asymmetric hysteresis in pulling experiments, in which varying tension (rather than temperature) first favours thermodynamically M-DNA, and then at later times, B-DNA.

2 Acknowledgements

We are grateful to J. Ricardo Arias-Gonzalez and Hanbin Mao for discussions and correspondence. We thank Carlos Bustamante, Michael Hagan, David Sivak and Steve Smith for discussions. We acknowledge the DOE for funding.

References

- [1] Smith, S.B., Cui, Y. & Bustamante, C. Overstretching B-DNA: The Elastic Response of Individual Double-Stranded and Single-Stranded DNA Molecules. *Science*, **271**, 795 (1996).
- [2] Cocco, S., Yan, J., Léger, J.-F., Chatenay, D. & Marko, J.F. Overstretching and force-driven strand separation of double-helix DNA. *Phys. Rev. E* **70**, 011910 (2004).
- [3] Cluzel, P., Lebrun, A., Heller, C., Lavery, R., Viovy, J.L., Chatenay, D. & Caron, F. DNA: An Extensible Molecule. *Science*, **271**, 792 (1996).
- [4] Storm, C. & Nelson, P.C. Theory of high-force DNA stretching and overstretching. *Phys. Rev. E* **67**, 051906 (2003).
- [5] Léger, J.-F., Romano, G., Sarkar, A., Robert, J., Bourdieu, L., Chatenay, D. & Marko, J.F. Structural Transitions of a Twisted and Stretched DNA Molecule. *Phys. Rev. Lett.* **83**, 1066 (1999).
- [6] Zhou, H.J. & Ou-Yang, Z.-C. Bending and Base-Stacking Interactions in Double-Stranded DNA. *Phys. Rev. Lett.* **82**, 4520 (1999).
- [7] Rouzina, I. & Bloomfield, V.A. Force-Induced Melting of the DNA Double Helix 1. Thermodynamic Analysis. *Biophys. J.* **80**, 882 (2001).
- [8] Williams, M.C., Rouzina, I. & Bloomfield, V.A. Thermodynamics of DNA Interactions from

Single Molecule Stretching Experiments. *Acc. Chem. Res.* **35**, 159 (2002)

[9] Williams, M.C. & Rouzina, I. Force spectroscopy of single DNA and RNA molecules. *Curr. Opin. Struct. Biol.* **12**, 330 (2002).

[10] Vladescu, I.D., McCauley, M.J., Rouzina, I. & Williams, M.C. Mapping the Phase Diagram of Single DNA Molecule Force-Induced Melting in the Presence of Ethidium. *Phys. Rev. Lett.* **95**, 158102 (2005).

[11] Mao, H.B., Arias-Gonzalez, J.R., Smith, S.B., Tinoco, I. & Bustamante, C. Temperature control methods in a laser tweezers system. *Biophysical Journal* **89**, 2, 1308 (2005).

[12] Poland, D. & Scheraga, H.A. Phase Transitions in One Dimension and the Helix-Coil Transition in Polyamino Acids. *J. Chem. Phys.* **45**, 1464 (1966).

[13] Fisher, M.E. Effect of Excluded Volume on Phase Transitions in Biopolymers. *J. Chem. Phys.* **45**, 1469 (1966).

[14] Kafri, Y., Mukamel, D. & Peliti, L. Why is the DNA Denaturation Transition First Order? *Phys. Rev. Lett.* **85**, 4988 (2000).

[15] Zimm, B.H. & Bragg, J.K. Theory of the Phase Transition between Helix and Random Coil in Polypeptide Chains. *J. Chem. Phys.* **31**, 526 (1959).

[16] SantaLucia, J. Jr. A unified view of polymer, dumbbell, and oligonucleotide DNA nearest-neighbor thermodynamics. *Proc. Natl. Acad. Sci. USA* **95**, 1460 (1998).

[17] Harris, S.A., Sands, Z.A. & Laughton, C.A. Molecular Dynamics Simulations of Duplex Stretching Reveal the Importance of Entropy in Determining the Biomechanical Properties of DNA. *Biophys. J.* **88**, 1684 (2005).

[18] Peyrard, M. & Bishop, A.R. Statistical mechanics of a nonlinear model for DNA denaturation. *Phys. Rev. Lett.* **62**, 2755 (1989).

[19] Dauxois, T., Peyrard, M. & Bishop, A.R. Entropy-driven DNA denaturation. *Phys. Rev. E* **47**, R44 (1993).

[20] Odijk, T. Stiff Chains and Filaments under Tension. *Macromolecules* **28**, 7016 (1995).

[21] Smith, S., Finzi, L. & Bustamante, C. Direct Mechanical Measurements of the Elasticity of Single DNA Molecules by Using Magnetic Beads. *Science* **258**, 1122 (1992).

[22] Rief, M., Clausen-Schaumann, H. & Gaub, H.E. Sequence-dependent mechanics of single DNA molecules. *Nature Struct. Bio.* **6**, 4, (1999).

[23] Williams, M.C., Wenner, J.R., Rouzina, I. & Bloomfield, V.A. Entropy and Heat Capacity of DNA Melting from Temperature Dependence of Single Molecule Stretching. *Biophys. J.* **80**, 1932 (2001).

[24] Metzler, R. & Ambjörnsson, T. Dynamic approach to DNA breathing. *J. Biol. Phys.* **31**, 331, (2005).

[25] Hwa, T., Marinari, E., Sneppen, K. & Tang, L.-h. Localization of denaturation bubbles in random DNA sequences *Proc. Natl. Acad. Sci.* **100**, 8, 4411 (2003).

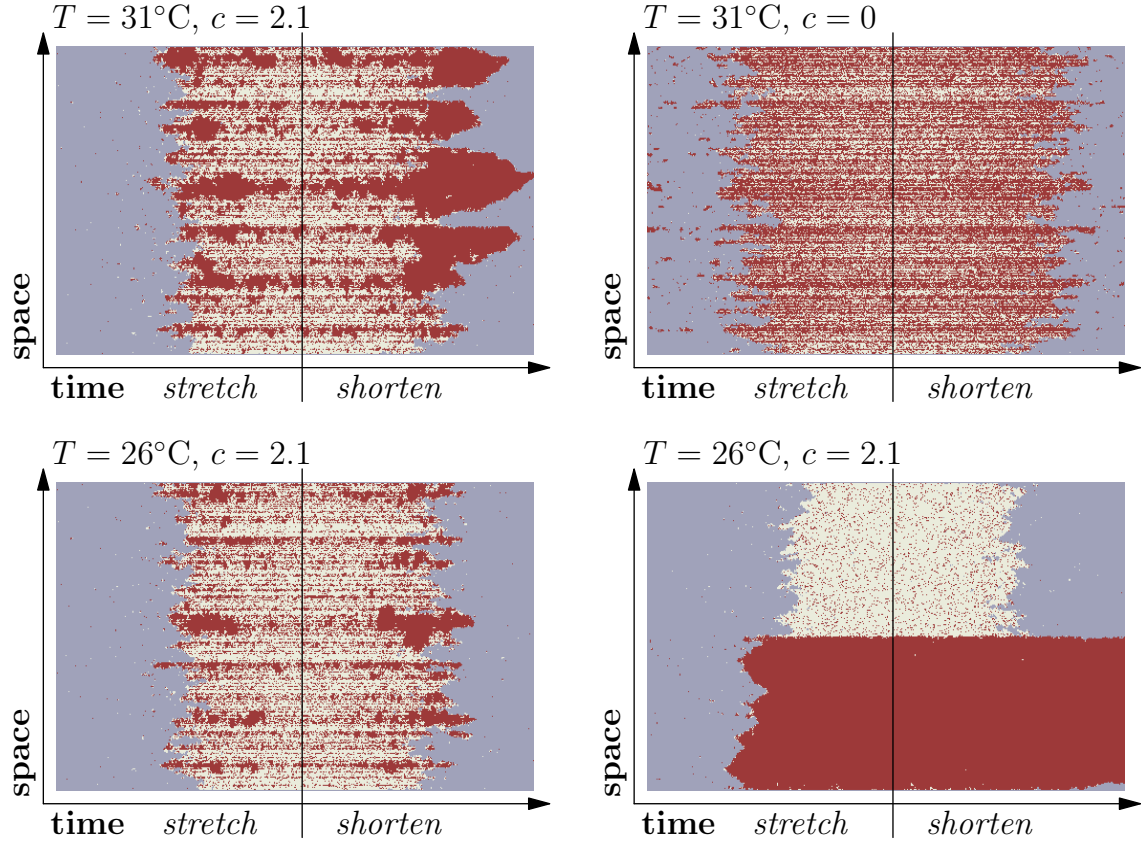


Figure 4: Microscopic configuration as a function of time for pulling simulations. We show space along the vertical (system size $N = 500$) and time along the horizontal for pulling simulations starting from zero tension and reversing at a force of 120 pN. Salt conditions are 50 mM. B-DNA is shown blue, S-DNA off-white, and M-DNA dark red. Each trajectory starts as mostly B-DNA and reaches an overstretched state consisting of some mixture of S- and M-DNA, depending on conditions. **Top row:** $T = 31^\circ\text{C}$, λ -phage DNA. Left panel: $c = 2.1$. The overstretched state contains large molten bubbles which develop in the high-force regime. These bubbles typically close only from their ends. Consequently, they are metastable on the timescale of the simulation, and persist long past the reversal point (vertical black line), preventing the shortening transition from reaching equilibrium. Right panel: $c = 0$. For zero loop exponent, no molten bubbles develop: M-DNA is mixed homogeneously with S-DNA and so is more easily replaced by B-DNA during shortening, even though the *equilibrium* fraction of M-DNA increases as c decreases. Consequently, no hysteresis is observed. **Bottom row:** $T = 26^\circ\text{C}$, $c = 2.1$. Left panel: λ -phage DNA. At a lower temperature, only small molten bubbles develop. These are relatively easily replaced by B-DNA during shortening, and lead to little hysteresis. Right panel: a system segregated into AT and CG halves. While almost no melting occurs in the CG section, the AT section melts entirely at large force, and remains molten on the time scale of the simulation. Thus hysteresis is a sensitive function of sequence.

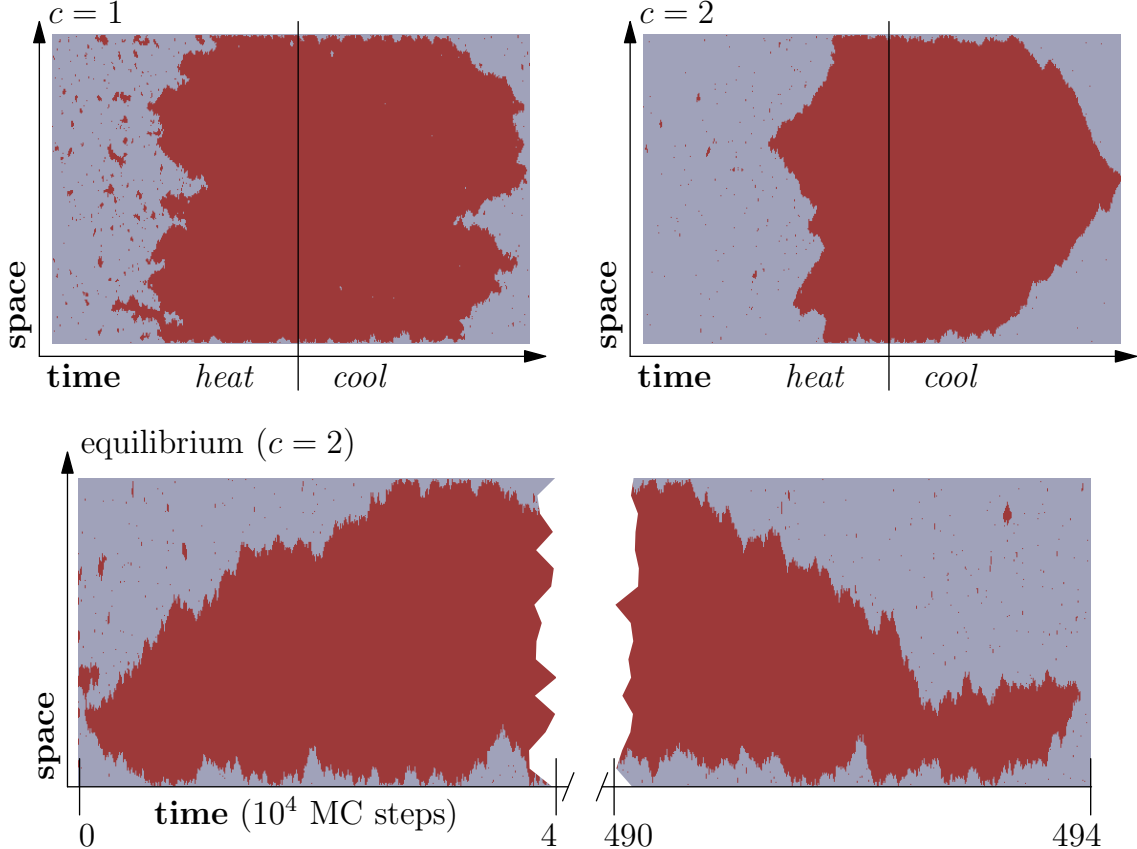


Figure 6: Illustration of the asymmetry of melting-hybridization dynamics. We allow only states B and M, and show microscopic configurations as a function of time for an homogeneous sequence. **Top panel:** heating-cooling cycle for $c = 1$ (left) and $c = 2$ (right). Starting from a low temperature, we increase the temperature linearly with time until well above the B-M coexistence temperature. Then we reverse the heating rate and cool the system until the original temperature is attained. Initially, as T increases, the size of the critical nucleus $\ell_{\text{c.n.}}$ shrinks (see text). M-DNA nucleates and grows, and bubbles coalesce when they meet. As T falls, the size of the critical nucleus increases, diverging at T_c . M-DNA becomes unstable. For small values of c (left panel), B-DNA can nucleate within the molten bubble, rendering the melting-hybridization dynamics roughly symmetric. For larger values of c (right panel), B-nucleation in large bubbles is suppressed kinetically: although thermodynamically unstable, the bubble closes not by many nucleation events, but by a collective ('spinodal') relaxation via domain wall drift over large distances. Thus the melting-hybridization dynamics is asymmetric. This asymmetry gives rise to melting-driven asymmetric hysteresis in pulling simulations, in which the varying control parameter is tension and not temperature. **Bottom panel:** equilibrium dynamics for $c = 2$ for a fixed temperature near coexistence. Here the critical nucleus spans the whole system, and bubbles open and close symmetrically. The dynamics is extremely slow: we show here the (abridged) time development of a single molten bubble, which takes many millions of MC steps to close. The loop exponent c endows space-time hyperbubbles with an hypersurface tension.